

Studies on the Kinetics of Na^+/H^+ Exchange in OK Cells: Introduction of a New Device for the Analysis of Polarized Transport in Cultured Epithelia

Danuta Krayer-Pawlowska, Corinna Helmle-Kolb, Marshall H. Montrose, Reto Krapf, and Heini Murer
Department of Physiology, University of Zürich, CH-8057 Zurich, Switzerland

Summary. The present study describes a new perfusion technique—based on the use of a routine spectrofluorometer—which enables fluorometric evaluation of polarity, regulation and kinetics of Na^+/H^+ exchange at the level of an intact monolayer. Na^+/H^+ exchange was evaluated in bicarbonate-free solutions in OK (opossum kidney) cells, a renal epithelial cell line. Na^+/H^+ exchange activity was measured by monitoring changes in intracellular pH (pH_i) after an acid load, using the pH-sensitive dye 2'7'-bis(carboxyethyl) 5-6-carboxy-fluorescein (BCECF). Initial experiments indicated that OK cells grown on a permeable support had access to apical and basolateral perfusion media. They also demonstrate that OK cells express an apical pH_i recovery mechanism, which is Na^+ dependent, ethylisopropylamiloride (EIPA) sensitive and regulated by PTH. Compared to resting conditions ($\text{pH}_i = 7.68$; $\text{pH}_o = 7.4$) where Na^+/H^+ exchange is not detectable, transport rate increased as pH_i decreased. A positive cooperativity characterized the interaction of internal H^+ with the exchanger, and suggests multiple H^+ binding sites. In contrast, extracellular $[\text{Na}^+]$ increased transport with simple Michaelis-Menten kinetics. The apparent affinity of the exchanger for Na^+ was 19 mM at an intracellular pH of 7.1 and 60 mM at an intracellular pH of 6.6. Inhibition of Na^+/H^+ exchange activity by EIPA was competitive with respect to extracellular $[\text{Na}^+]$ and the K_i was 3.4 μM . In conclusion, the technique used in the present study is well suited for determination of mechanisms involved in control of epithelial cell pH_i and processes associated with their polarized expression and regulation.

Key Words brush border membrane · amiloride · tissue culture · intracellular pH · fluorescence

Introduction

Cultured epithelial cells have been shown to express apical and/or basolateral Na^+/H^+ exchange (Montrose, Friedrich & Murer, 1987; Haggerty et al., 1988; Casavola, Helmle-Kolb & Murer, 1989; Helmle-Kolb et al., 1990a; Montrose & Murer, 1990a). The characteristics of these exchangers vary both kinetically (amiloride sensitivity) and in terms of hormonal regulation (Haggerty et al., 1988; Casavola et al., 1989), suggesting the presence of several distinct Na^+/H^+ exchangers which may be expressed in these epithelial cells. We have previously developed

microfluorometric techniques for the determination of polarized proton transport systems in single cultured epithelial cells within a monolayer (Montrose et al., 1987; Montrose & Murer, 1990a,b). Ideally, these measurements should be compared to population measurements made under the same conditions, since the use of suspended cells (or cells on an impermeant support) may compromise the ability to discriminate the presence of multiple transporters. For this reason, we have defined a spectrofluorometric technique—based on the use of a routine spectrofluorometer—which allows determination of polarized transport functions in a whole cell population grown in monolayer configuration. To establish this technique, we have used a simple cell system which is known to express only apical Na^+/H^+ exchange (OK cells) (Helmle-Kolb et al., 1990a; Montrose & Murer, 1990a). In addition to establishing the technique, this paper characterizes kinetic features of the OK cell Na^+/H^+ exchanger which have not been previously determined and which will be important for the further understanding of the mechanisms of hormonal regulation of this exchanger and the homology of the OK cell exchanger to that in the renal proximal tubule.

Materials and Methods

MATERIALS

Nigericin was obtained from Calbiochem (Luzern, Switzerland). BCECF-AM¹ was purchased from Molecular Probes (Eugene,

¹ Abbreviations: pH_o , extracellular pH; pH_i , intracellular pH; HEPES, 4-(2-hydroxyethyl)-1-piperazine ethane-sulfonic acid; BCECF, 2'7'-bis(carboxyethyl)5-6-carboxy-fluorescein-acetoxymethyl ester; EIPA, ethylisopropylamiloride; PTH, synthetic bovine 1-34 parathyroid hormone; TMA^+ , tetramethylammonium; J^{H} , transmembrane proton flux; $[\text{H}^+]_i$, intracellular proton concentration; β , intracellular buffer capacity.

Table. Composition of perfusion solutions (concentration given in mM)

Solution	NaCl	TMACI	KCl	CaCl ₂	MgSO ₄	Phosphate	Glucose	HEPES
Na medium ^d	130	—	4	1	1	1(1.75 Na ⁺)	18	20 ^a
TMACI medium ^d	—	130	4	1	1	1(1.75 TMA ⁺)	18	20 ^b
K-clamp medium	20	—	110	1	1	1(1.75 TMA ⁺)	18	20 ^c

^a pH titrated to pH 7.4 with NaOH (osmolality: 310 mosmol/kg).

^b pH titrated to pH 7.4 with TMAOH (osmolality: 310 mosmol/kg).

^c pH titrated from 6.5 to 7.72 with NaOH (osmolality: 310 mosmol/kg). To calibrate BCECF intracellularly, K-clamp media of varying pH contained additionally 0.5 μM nigericin.

^d In some experiments Na- and TMACI-media were blended together to give intermediate Na⁺ concentrations

OR). EIPA was a generous gift of Dr. G. Burckhardt and T. Friedrich (Max Planck Institute for Biophysics, Frankfurt a.M. (FRG)). PTH was from Bachem (Bubendorf, Switzerland). All other chemicals were purchased either from Sigma (St. Louis, MO) or Fluka (Buchs, Switzerland).

COMPOSITIONS OF SOLUTIONS

All experiments were performed in the presence of HEPES-buffered, bicarbonate-free solutions at 25°C. The composition of the solutions is given in the Table.

CELL CULTURE

The OK cells used in the present study were from the same subclone as described previously (Helmle-Kolb et al., 1990b). They were maintained in a humidified 5% CO₂/95% air atmosphere at 37°C in 1:1 Dulbecco's modified Eagle's medium (DMEM): Hams F12, supplemented with 2 mM glutamine, 50 IU/ml penicillin, 50 μg/ml streptomycin, 20 mM HEPES and 10% fetal calf serum. Cells were subcultured for serial passage and experimental use from confluent monolayers grown in 25-cm² culture flasks, as described previously (Malmström, Stange & Murer, 1988). For experiments, cells were seeded onto collagen-coated "filterslips" at a density of 2 × 10⁵ cells/filterslip and maintained in tissue culture as described earlier (Montrose & Murer, 1990b). Filterslips (Teflon filters attached to a plastic coverslip) were prepared essentially as described by Montrose and Murer (1990b), except that the size of the plastic coverslip was adjusted to the dimensions of the perfusion cuvette (here: 9 × 22 mm) and the hole (here: 3.5 × 6.6 mm) was centered in the lower part of the coverslip. In this way the fluorescence signal was collected only from cells on the permeant portion of the filter support.

FLUORESCENT MEASUREMENT OF pH_i

Intracellular pH was measured using the fluorescent dye BCECF. Cells on filterslips were loaded with BCECF by exposure for 60 min to 8.3 μM (25 μmol total) of the acetoxymethyl ester at room temperature in "Na medium." For experiments using nigericin, dye loading was performed in "K-clamp medium" containing 5 μM nigericin. After the dye-loading interval, the filterslip with the confluent monolayer was inserted into a specially designed perfusion cuvette (*see below*), which was placed into a thermoregulated chamber in a spectrofluorometer (Shimadzu RF-5000). The perfusion cuvette was connected to perfusion tubing (*see below*)

and cells on filterslips were independently superfused with Na medium from both the apical and basolateral side (flow rate: 1 ml/min each). Using computerized scanning monochromators fluorescence was measured alternately at 500 and 455 nm excitation (bandwidth 5 nm) and at a constant emission wavelength of 530 nm (bandwidth 15 nm). On-line calculation of fluorescence ratios from these two excitation wavelengths was used to measure pH_i. To minimize photodynamic damage and extend the duration of experiments, fluorescence light from the 150 W xenon lamp of the spectrofluorometer was attenuated with a 12% transmitting neutral density filter, and an electronic shutter was placed into the light path, to block the illumination whenever desired.

PERFUSION CUVETTE

Figure 1 specifies the technical details of the perfusion cuvette used for independent perfusion of cells on filterslips from both the apical and basolateral side. The cuvette is made in two asymmetric halves which are connected together by screws during an experiment. Each half is equipped with a cylindrical perfusion space (block A: 95 μl; block B: 65 μl) sealed by a quartz window on the external surface and narrowing to a tunnel facing the filterslip. The dimensions (approx. 1.8 × 3.5 mm) and angle of the tunnel are such that excitation light only impinges on a restricted area of cells on the permeant portion of filter support. To minimize unstirred layers, the tunnel is constructed as short as possible, and perfusion inlets are placed as close as possible to the internal filterslip-mounting surface of each half block. Perfusion outlets are located within the perfusion chamber; this design permits rapid exchange of different solutions (in ~2 sec). In all experiments, cells are continuously superfused at a flow rate of ~1 ml/min. To minimize light scatter, the cuvette is made of black Ertacell plastic, and the filterslip is mounted at an angle of 60° to the excitation beam. Rubber gaskets (0.25 mm thickness) placed on each side of the filterslip prevent leakage of perfusion fluids.

PERFUSION SYSTEM

As described previously (Montrose et al., 1987), multiple perfusion solutions were kept at equal hydrostatic pressure for gravity-driven perfusion. Selection of perfusates was made via manual valves connected to a Lucite manifold.

CALIBRATION OF THE BCECF FLUORESCENCE SIGNAL

Calibration of intracellular BCECF was performed by monitoring the 500/455 nm excitation ratio at various values of pH_i. pH_i was set approximately equal to predetermined extracellular pH values

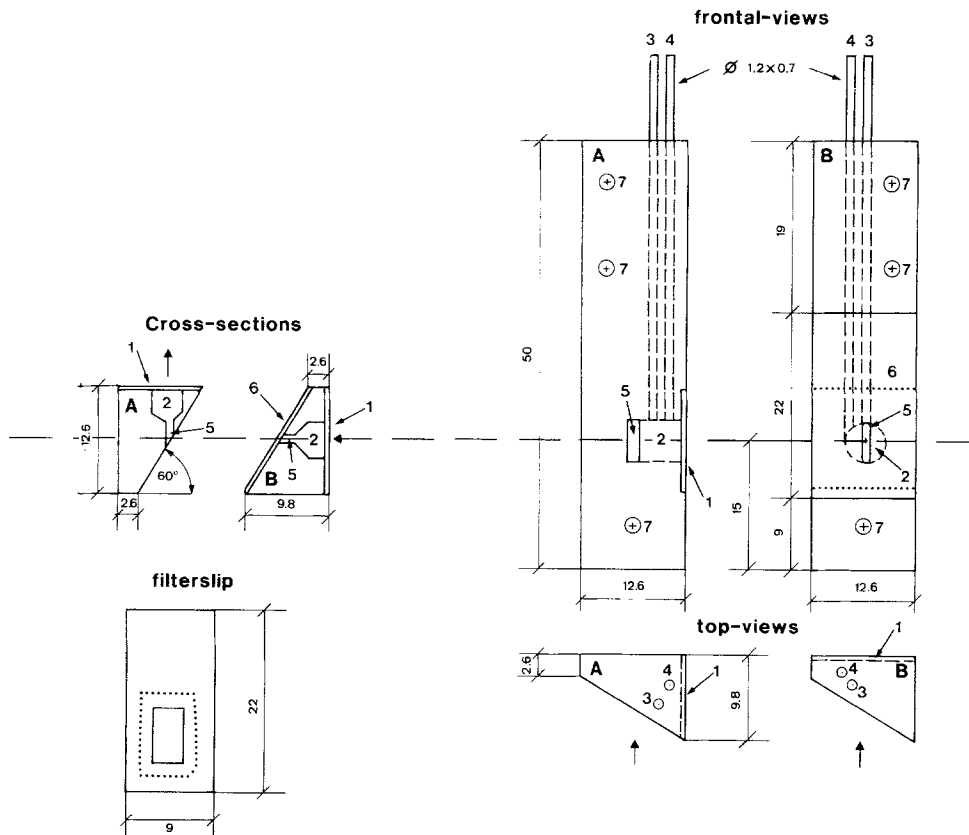


Fig. 1. Construction of perfusion cuvette, three different views of halfblock A and halfblock B are given (all dimensions in the diagram are in millimeters): the half-blocks (A + B) can be placed together by three screws (7). Block B contains a relieved area (6) to accommodate the filterslip (0.25 mm deep). Block B is oriented towards the excitation light source; block A is towards emission: (1) quartz windows (0.5 mm thickness); (2) perfusion chamber (cylindrical, 4 mm diameter); (3) perfusion inlets (stainless steel), reaching the top of the access ports (5); (4) perfusion outlets (stainless steel), reaching the top of perfusion chambers (2); (5) horizontal access port, permitting the access of perfusion fluid to the monolayer grown on filterslip. The *cross-sections* are at the level of the perfusion chamber and show the position of the filterslip (6) as well as the design of the perfusion chamber (2); the arrows near the quartz windows determine excitation and emission light, respectively. The *top-views* show the position of the perfusion inlets (3)/outlets (4) as well as of the quartz windows (1); not on the same planes, *see frontal views*). The arrows in the top views indicate the direction for the *frontal-views*. The dashed lines define the position of the quartz windows (*top-views*) or perfusion compartments (*frontal-views*) which are on different section planes and thus not visible. In the frontal view of block B the dotted lines define the size of quartz window at the outer surface. The *filterslip* (0.25 mm thickness) contains a rectangular whole covered by the Teflon filter (dotted area). For further details *see text*

using the K⁺/nigericin technique (Thomas et al., 1979). OK-cell monolayers grown on filterslips were dye loaded in K-clamp medium (pH_o = 7.4) containing 5 μM nigericin prior to perfusion, because introduction of the ionophore via perfusion is slow (Montrose et al., 1987). After the dye-loading interval (1 hr), OK-cell monolayer filterslips were transferred to the perfusion cuvette, placed into the spectrofluorometer and perfused with K-clamp media of varying pH, with 0.5 μM nigericin. pH_o was then varied from 7.72 to 6.65 in steps of 0.3 pH units.

INTRACELLULAR BUFFER CAPACITY

Intracellular buffer capacity (β) was determined using the technique of NH₃/NH₄⁺ addition and partial removal as described by Boyarsky, Ganz and Boron (1988). Briefly, exposure to NH₄Cl (20 mM) results in a rapid cellular alkalization as NH₃ equilibrates cross the cell membrane, and subsequent lowering of extra-

cellular NH₃ concentration to 10, 5 and 0 mM (in the continued absence of extracellular Na⁺ to inhibit Na⁺/H⁺ exchange) induces a stepwise fall in pH_i, due to loss of NH₃. Cellular buffering capacity was calculated from these pH_i steps precisely as described by Weintraub and Machen (1989).

Results

FLUORESCENCE INTENSITY AS A FUNCTION OF INTRACELLULAR pH

OK cells were grown on a permeable Teflon filter, loaded with BCECF and mounted in a special cuvette that allows independent perfusion of the apical and basolateral aspects of the cells. Figure 2a shows a typ-

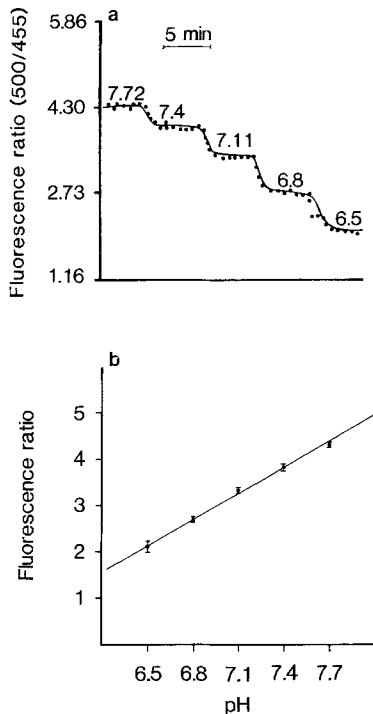


Fig. 2. Calibration of intracellular BCECF. OK cells were loaded with $25 \mu\text{M}$ BCECF/AM as described in Materials and Methods, mounted into the perfusion cuvette, and the fluorescence excitation ratio (500/455 nm) was measured. (a) A typical time course is presented in which OK-cell monolayers were perfused with different K-clamp media ($+0.5 \mu\text{M}$ nigericin) of the pH indicated. (b) Dependence of fluorescence excitation ratio on pH_i . Data points were derived from experiments similar to that of a. Mean \pm SE of three experiments are presented

ical calibration experiment of BCECF-loaded OK cells in this configuration. The fluorescence ratio from dual excitation wavelengths (*see* Materials and Methods) was plotted *vs.* time, when pH_i was manipulated by exposing cells to K-clamp media (plus nigericin) of different pH values. The calibration curve shown in Fig. 2b was derived from the result in three different OK-cell monolayers. As illustrated, pH_i was a linear function (correlation coefficient, 0.999) of the excitation ratio over the pH_i range of 6.5 to 7.7. Similar observations have been reported by others (Alpern, 1985; Kurtz, 1987; Boyarsky et al., 1988; Nord, Brown & Crandall, 1988; Weintraub & Machen, 1989; Montrose & Murer, 1990b). Therefore, this calibration curve was used to convert the fluorescence ratio (500/455) into pH_i values.

BASIC PROPERTIES OF OK CELLS IN CONFLUENT MONOLAYERS

We next examined whether OK cells grown to confluency on filterslips (*see* Materials and Methods)

and built into the perfusion cuvette display a Na^+ -dependent pH_i regulatory mechanism similar to that reported in single cell analysis (Helmle-Kolb et al., 1990a; Montrose & Murer, 1990a). BCECF-loaded cells initially perfused with HEPES-buffered, bicarbonate-free Na medium, were subjected to a brief exposure to 20 mM NH_4Cl (NH_4Cl prepulse (Boron & DeWeer, 1976)). After 5–7 min NH_4Cl was removed and replaced by the Na^+ -free solution “TMACl medium.” This resulted in a cellular acid load due to the NH_3 loss. As soon as cells reached a stable acid pH_i , cells were returned to Na medium and the rate of pH_i recovery was recorded. As shown in Fig. 3, abrupt removal of NH_4Cl from the superfusion solution rapidly acidified these cells. In Na^+ -free medium, cells remain acidified. Upon symmetrical addition of Na^+ (Fig. 3a), pH_i recovered from this acid load and achieved a stable pH_i not significantly different from base line (*data not shown*). Consistent with our previous observations (Helmle-Kolb et al., 1990a; Montrose & Murer, 1990b) steady-state pH_i values of OK cells superfused with HEPES-buffered bicarbonate-free Na medium were quite high and averaged 7.68 ± 0.05 ($n = 20$). This suggests that removal of $\text{HCO}_3^-/\text{CO}_2$ compromises the pH-regulatory behavior of OK cells, as observed previously (Montrose & Murer, 1990b).

To further assess the properties of OK cells in the new perfusion system, OK-cell monolayers were examined for polarized expression of pH_i recovery from an acid load. In the experiment shown in Fig. 3b acidified cells were first exposed to Na^+ from the basolateral compartment. Upon addition of Na^+ to the basolateral surface of OK cells, pH_i recovered at a very slow rate compared to the pH_i recovery when Na^+ was subsequently present at the apical and basolateral surface of OK cells. The rate in pH_i recovery after basolateral addition of Na^+ only was indistinguishable from that in the complete absence of Na^+ (Fig. 3b). As expected, when Na^+ is given first to the apical compartment, pH_i recovered immediately (Fig. 3b, dashed experimental trace and dashed boxes for perfusion condition). This defines that the OK-cell monolayer remains polarized and shows apical Na^+/H^+ exchange only, and that the new perfusion system functionally separates apical versus basolateral compartments. To avoid the presence of ionic gradients across the monolayer, solution changes were made symmetrically (in both the apical and basolateral perfusates) for most of the subsequent studies. Furthermore, in subsequent experiments (Figs. 5–7), only the Na^+ -dependent pH_i recovery was considered as Na^+/H^+ exchange, i.e., any rate in the absence of Na^+ (TMA^+ ; usually very small, *see* e.g. Fig. 3a and b) was subtracted from that after addition of Na^+ .

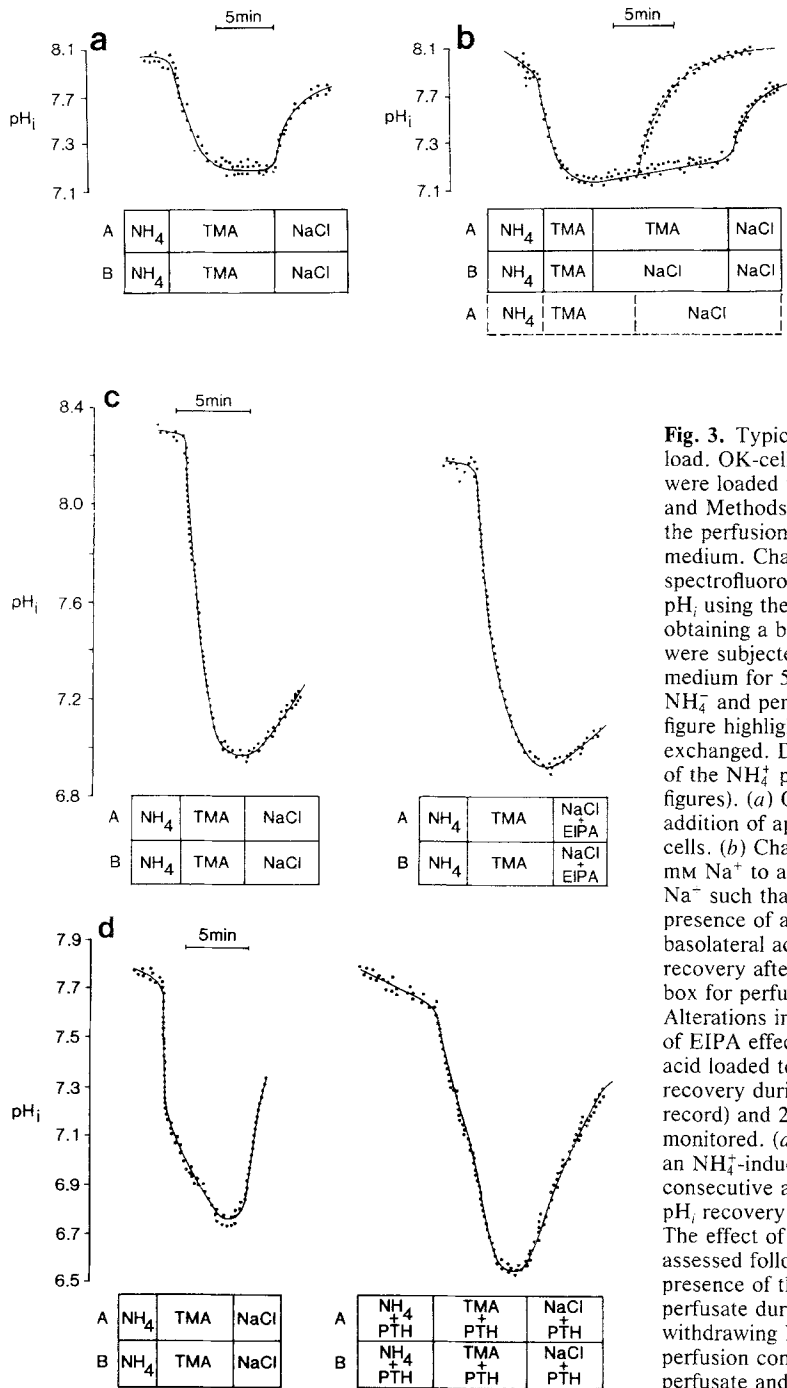


Fig. 3. Typical responses of OK-cell monolayers to an acid load. OK-cell monolayers grown to confluency on filterslips were loaded with 25 μM BCECF/AM as detailed in Materials and Methods. After dye loading, filterslips were mounted into the perfusion cuvette and were allowed to re-equilibrate in Na medium. Changes in pH_i were determined by excitation ratio spectrofluorometry. The ratio at 500/455 nm was converted to pH_i using the calibration curve shown in Fig. 2. After obtaining a baseline tracing (resting pH_i determination) cells were subjected to an acid load due to NH_4^+ (20 mM NH_4 in Na medium for 5–7 min). Acid loading was initiated by removal of NH_4^+ and perfusion with TMA/Cl medium. Bars beneath the figure highlight where indicated solutions in the cuvette were exchanged. Data presentation is started during the last 2 min of the NH_4^+ prepulse (this convention is followed in all figures). (a) Change in pH_i resulting from simultaneous addition of apical and basolateral 140 mM Na^+ to acidified cells. (b) Change in pH_i resulting from ordered addition of 140 mM Na^+ to acidified cells. Acid-loaded cells were exposed to Na^+ such that basolateral addition of Na^+ (in the continued presence of apical TMA⁺) was followed by apical and basolateral addition of Na^+ . The dashed trace indicates pH_i recovery after giving Na^+ to the apical perfusate only (dashed box for perfusion condition in apical compartment). (c) Alterations in pH_i recovery rate due to 5 μM EIPA. For study of EIPA effects within one monolayer, cells were repeatedly acid loaded to the same acidified pH_i . Changes in pH_i recovery during perfusion with 28 mM Na^+ (control; left record) and 28 mM Na^+ plus EIPA (right record) were monitored. (d) Effect of 10^{-8} M PTH on recovery of pH_i from an NH_4^+ -induced acid load. Cells were subjected to two consecutive acid loads. Under control conditions (left record) pH_i recovery was measured in the presence of 140 mM Na^+ . The effect of PTH on transport rate (right record) was assessed following a 15-min incubation period in the continued presence of the hormone (i.e., PTH was added to the perfusate during acid load imposed by applying and withdrawing NH_4^+ and was present thereafter). For the perfusion conditions given in the boxes, A defines apical perfusate and B, basolateral perfusate

The effect of EIPA (a relatively specific inhibitor of Na^+/H^+ exchange (Vigne et al., 1983, 1984)) on this Na^+ -dependent pH_i recovery is shown in Fig. 3c. In this experiment pH_i recovery in response to the addition of 28 mM Na^+ to the apical and basolateral surface of the monolayer was analyzed both in the absence and presence of 5 μM EIPA. To facilitate comparison, pH_i recovery was recorded from a similar initial pH_i . The results show, that 5 μM EIPA

inhibited Na^+ -dependent pH_i recovery. These features are also similar to those observed previously (Helmle-Kolb et al., 1990a; Montrose & Murer, 1990a) and suggest that pH_i recovery is due to the operation of Na^+/H^+ exchange. 5 μM EIPA had no effect on pH_i after acidification in the absence of Na^+ (TMA⁺ medium; data not shown).

To confirm that the new perfusion system has adequate sensitivity to detect regulatory changes in

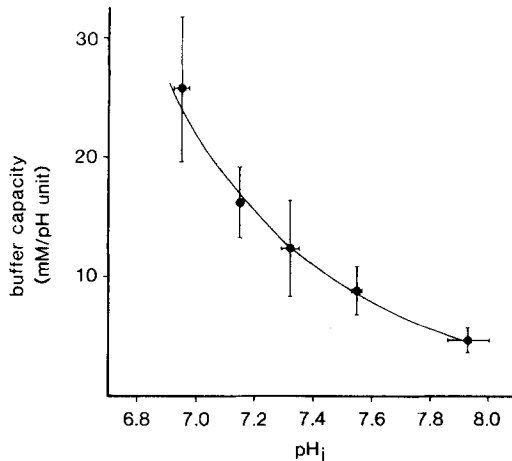


Fig. 4. pH_i dependence of intracellular buffer capacity in OK-cell monolayers. β was determined as detailed in Materials and Methods in eight monolayers exposed to a concentration range of 0–20 mM NH_4Cl in TMAcI medium ($\text{pH}_i = 7.4$). The reference pH_i to which calculated values of β were related was taken to be the midpoint of the range over which pH_i varied after exposure to or removal of NH_4Cl . Raw data from 23 individual data points were grouped into intervals of 0.2 pH units and were plotted as mean buffer capacity (\pm SE; vertical bars) vs. mean pH_i values (\pm SE; horizontal bars) in each pH interval

transport, we compared the PTH-dependent inhibition of transport activity derived from single cell analysis (Helmle-Kolb et al., 1990a) with the current technique. Figure 3d represents a typical experimental tracing of Na^+ -dependent pH_i recovery in the absence and presence of 10^{-8} M PTH. According to a protocol established in our laboratory (Helmle-Kolb et al., 1990b) PTH effects on pH_i recovery were evaluated after a 15-min exposure of cells to PTH in the continued presence of the hormone. As observed previously, PTH inhibited Na^+/H^+ exchange (27% inhibition), when applied from the apical and basolateral side, thus demonstrating that these OK-cell monolayers preserved their PTH responsiveness and that the system can detect such responses.

INTRACELLULAR BUFFER CAPACITY

In order to allow calculation of proton fluxes via Na^+/H^+ exchange (as opposed to $\Delta \text{pH}_i/\text{min}$) the intracellular buffer capacity (β) in OK-cell monolayers was determined as described in Materials and Methods. In Fig. 4, measured buffer capacity is plotted vs. pH_i . Buffer capacity depends significantly on pH_i over the tested pH_i range (6.8–8.0). Buffer capacity was 4.6 mM/pH unit at pH_i 7.9, increased to 12.3 mM/pH unit at pH_i 7.32, and to 26 mM/pH unit at pH_i 6.95, respectively. In addition to the value

of β shown in Fig. 4, a β value was determined at $\text{pH}_i = 6.74 \pm 0.02$ ($n = 5$) following removal of 20 mM NH_4Cl from cells previously acidified by NH_4Cl prepulses. This value of 166.04 ± 6.29 mM/pH unit at this very acidic pH_i value was required for later kinetic analyses and could not be obtained by the standard protocol which was used to generate the other values.

RELATIONSHIP BETWEEN pH_i AND Na^+/H^+ EXCHANGE ACTIVITY

To evaluate the pH_i dependence of Na^+/H^+ exchange in OK-cell monolayers the response of OK cells to progressively larger acid loads (imposed by 10, 20, 30, 40, and 50 mM NH_4Cl) was measured. For the analysis of pH_i recovery, a protocol similar to that of Fig. 3a was used and transmembrane proton flux rates (J^{H}) were calculated from multiplying pH_i/min rates by the β at the starting pH_i . Figure 5a represents the relationship between pH_i and rate of Na^+/H^+ exchange. As illustrated, the rate of exchange was highest at lowest pH_i values. With increasing the starting pH_i , the rate of pH_i recovery fell progressively to undetectable values at pH_i 7.5. The data presented in Fig. 5a indicate that the rate of acid extrusion is at least 10-fold stimulated as the pH_i is decreased from 7.5 to 6.5. When the data are replotted vs. proton concentration ($10^{-\text{pH}}$) (Fig. 5b), the dependence of flux on $[\text{H}^+]_i$ is shown to be "sigmoidal." When this data is analyzed by a nonlinear least squares fit to the Hill equation, the best fit parameters indicate a Hill coefficient of 4.0 and half maximal transport at a pH_i of 6.0 (analysis not shown).

Na^+ DEPENDENCE OF pH_i RECOVERY

It has been demonstrated previously in OK cells that extracellular Na^+ activates Na^+/H^+ exchange with Michaelis-Menten kinetics (Montrose & Murer, 1990a). It has not been defined whether changes in pH_i alter the apparent affinity (K_m) for Na^+ at the extracellular surface, therefore we have evaluated the K_m at pH_i 6.6, and pH_i 7.1. The Na^+ -activation kinetics of the apical Na^+/H^+ exchange were determined by measuring the rate of pH_i change upon readdition of varying concentrations of Na^+ (5, 14, 28, 70, and 140 mM Na^+) to acidified cells. Experiments were such that the recovery rate was defined first in the presence of 140 mM Na^+ and then in the presence of varying Na^+ concentrations. The final pH_i recovery was measured in the presence of 140 mM Na^+ to exclude fatigue effects over the time of

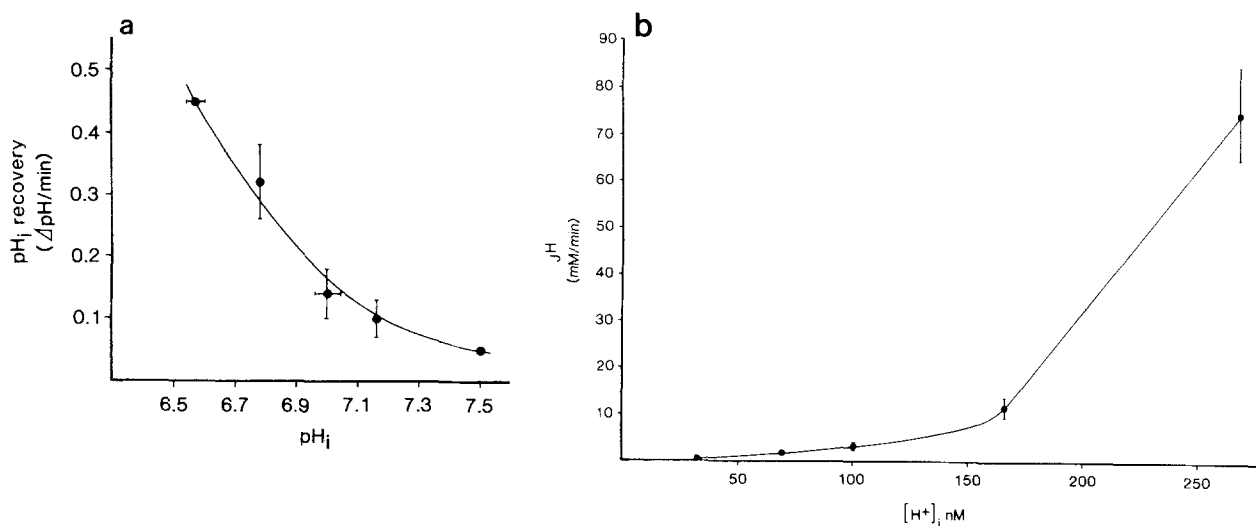


Fig. 5. pH_i dependence of Na⁺/H⁺ (ΔpH/min) exchange activity. (a) Rate of Na⁺/H⁺ exchange as a function of initial pH_i. BCECF-loaded cells within one monolayer were acidified to different pH_i values by sequential exposure to Na medium containing 10, 20, 30, 40 and 50 mM NH₄Cl. After simultaneous removal of external NH₄⁺ and external Na⁺ (TMA⁺ medium), initial rates of pH_i recovery due to subsequent addition of 140 mM Na⁺ were measured as detailed in Fig. 3a. For purposes of data presentation, the resultant pH_i recovery rates were compiled into 0.2 pH_i unit groups (4–6 determinations for each group) and are plotted as means ±SE versus means of pH_i at 0.2 pH unit intervals. pH_i recovery rates are corrected for Na⁺-independent pH_i recovery; i.e., recovery rate in TMA⁺ medium was absent or minimal. Results are derived from seven experiments. (b) Representation of data of a by plotting J^H (obtained from the product of dpH_i/dt and β at appropriate pH_i values) against intracellular H⁺ concentration ([H⁺]_i).

data acquisition. Figure 6a presents the proton flux rates at the respective pH_i values. A Hanes-Woolf transformation of this data is shown in Fig. 6b, and the K_m and V_{max} parameters from the least squares fit to this transformed data are used to define the solid lines in both Fig. 6a and b. As shown in Fig. 6b, the results suggest that both the V_{max} and K_m change as a function of pH_i, such that both the K_m and the V_{max} are higher at the lower pH_i.

INTERACTION OF EIPA WITH THE Na⁺/H⁺ EXCHANGE SYSTEM

In order to evaluate the EIPA inhibition of the Na⁺/H⁺ exchange shown in Fig. 3c in more detail, we tested the influence of two different concentrations of this compound (5 and 10 μM) on Na⁺-dependent pH_i recovery at 14, 28 and 140 mM extracellular Na⁺. Figure 7 summarizes the magnitude of EIPA inhibition of transport activity determined at a starting pH_i of 6.83. As demonstrated in Fig. 7 the EIPA inhibition is released as the Na⁺ concentration is increased. The addition of 5 μM EIPA reduces the initial rate of Na⁺-dependent pH_i recovery at 14, 28 and 140 mM Na⁺ by 56, 39, and 3%, respectively. In comparison, 10 μM EIPA diminishes transport rate at 14, 28 and 140 mM Na⁺ by 78, 81 and 59%, respectively. As shown in the inset, kinetic analysis of the

inhibition using a Dixon replot of data measured at 14 and 140 mM Na⁺ indicates that EIPA competes with Na⁺ for its binding to the Na⁺/H⁺ exchanger. From the Dixon representation the inhibitor constant was estimated to be 3.4 μM. EIPA at 5 and 10 μM concentration has no effect on pH_i after acidification in the absence of Na⁺ (TMA⁺-medium; data not shown).

Discussion

Several techniques are currently available for measuring pH_i in cells (Frelin et al., 1988; Madhus, 1988). Optical techniques offer the advantages of rapid response time, excellent pH_i sensitivity and high signal-to-noise ratio. In this study we describe a new perfusion technique allowing continuous fluorometric evaluation of pH_i-regulation in cell monolayers grown on a permeable support in response to solution changes in the apical or basolateral compartment; this technique is based on the use of a routine spectrofluorometer. The pH_i-sensitive dye BCECF was used to monitor pH_i in these cell monolayers. Several parts of the new system were critical for success. To counter the problem of dye bleaching, which would limit data acquisition, we introduced a neutral density filter in the light path, to

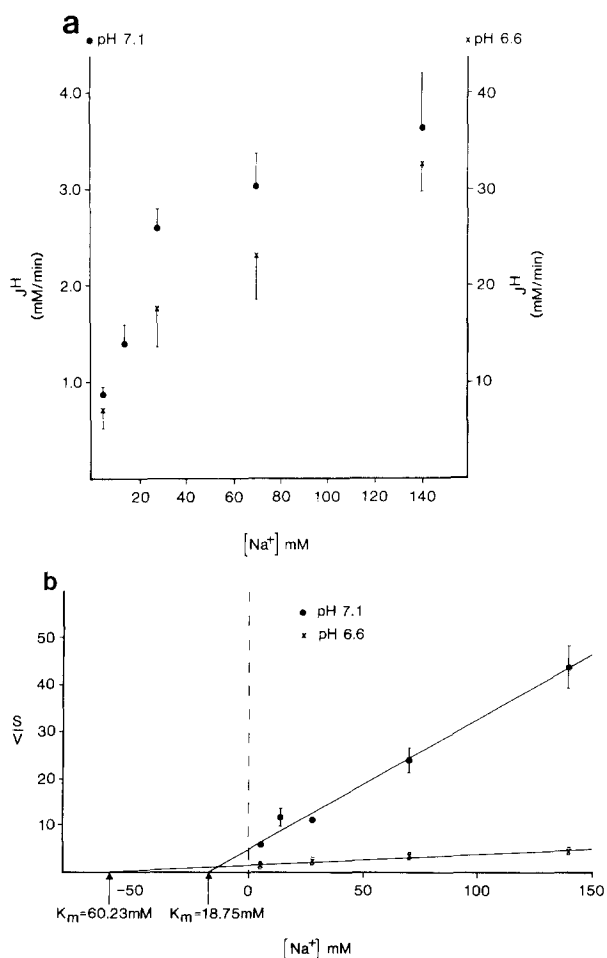


Fig. 6. Affinity of Na^+ at the extracellular surface of the Na^+/H^+ exchanger at $\text{pH}_i = 6.6$ and $\text{pH}_i = 7.1$. Experiments were performed according to protocol of Fig. 3a. Application and withdrawal of 20 mM NH_4Cl for different time intervals caused pH_i to decrease to desired values. Rates of recovery from an NH_4 -induced acid load were measured in response to 5, 14, 28, 70 and 140 mM Na^+ in the apical and basolateral perfusion media. To examine the effect of a series of different Na^+ concentrations within one monolayer, cells were repeatedly acidified to respective acid pH_i values. (a) Representation of average initial rate of Na^+ -induced transmembrane proton flux (J^{H}) as a function of different external Na^+ concentrations. J^{H} was calculated as described in the legend to Fig. 5, using the value for β determined for corresponding values of pH_i . (b) Hanes-Woolf plot of data shown in a. Regression lines were fit using a least squares fit analysis. At $\text{pH}_i = 6.6$, the best fit parameters were $K_m = 60.23$ mM and $V_{\text{max}} = 41.9$ mM H^+/min , while at $\text{pH}_i = 7.1$, the best fit parameters were $K_m = 18.75$ mM and $V_{\text{max}} = 3.6$ mM H^+/min . Means \pm SE are presented. Values are related to Na^+ -dependent pH_i recovery only (see Fig. 5)

attenuate the excitation light. In addition, we placed an electronic shutter in the light path to fully block light whenever continued data collection was not required (i.e., pH_i transitions during NH_4^+ prepulse, etc.). Several features also assured rapid solution

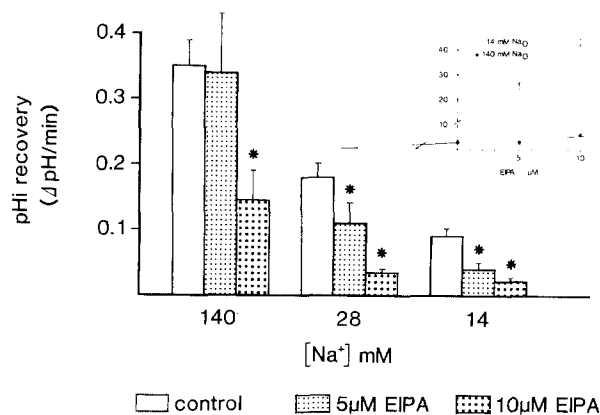


Fig. 7. Properties of inhibition of Na^+/H^+ exchange by EIPA. OK-cell monolayers were acidified by NH_4 -prepulse technique to a pH_i of 6.83. Measurements of pH_i recovery from this acid load were performed as detailed in Fig. 3a at 14, 28 and 140 mM Na^+ , respectively. For evaluation of effects of varying concentrations of EIPA (5 and 10 μM) on transport rate acidified cells were returned to Na^+ -containing perfusion medium supplemented with the respective inhibitor concentration. The experimental scheme for determining the interaction of EIPA with Na^+/H^+ exchange was such that at any Na^+ -concentration tested cells were first observed during pH_i recovery measured in the absence of EIPA (control) and following reacidification in the presence of EIPA. This sequence was continued either at a different Na^+ -concentration or at another EIPA concentration. In this way the only variable within one experiment was either the EIPA concentration or the Na^+ concentration. Values are related to Na^+ -dependent pH_i recovery only (see Fig. 5). *Main panel:* rate of pH_i recovery in response to varying extracellular Na^+ concentrations as a function of the EIPA concentration. Each point represents the mean \pm SE of at least three determinations. *Inset:* Dixon plot of EIPA inhibition of Na^+/H^+ exchange activity at 14 and 140 mM extracellular Na^+

changes during experiments: Inlet ports for perfusion solutions were mounted close to the cell monolayer and outlet ports further away in the perfusion chamber. The size of the tunnel giving access of fluid and light to the monolayer was kept as small as possible and was a compromise between unstirred layer problems and intensity of light to give a good signal-to-noise ratio.

The experiments summarized in Figs. 2 and 3 are used only to validate the present technique for the evaluation of pH_i regulation in polarized epithelial cell monolayers. To calibrate the probe fluorescence as a function of the pH_i , we used the procedure of Thomas et al. (1979), equilibrating H^+ and K^+ with the H^+-K^+ ionophore nigericin. In the presence of high external K^+ , BCECF loaded cells showed a linear relationship between fluorescence ratio and pH_i over the pH range 6.5–7.7 (Fig. 2). The experimental tracings shown in Fig. 3 address the issue of functional integrity of Na^+/H^+ exchange in OK cell monolayers under the present experimental

conditions. Data on p*H*_i transitions in response to an NH₄ prepulse demonstrate that the perfusion technique used in our fluorometric determinations of p*H*_i regulation is suitable to accurately measure rapid p*H*_i changes. Since the response due to any solution change in either of the two compartments (apical *vs.* basolateral) was rapid in onset (e.g. Fig. 3*b*), inaccuracy due to unstirred layers in the perfusion cuvette seems to be minimal. Averaging data measured under control conditions (protocol as in Fig. 3*b*; polarity of expression of Na⁺/H⁺ exchange) (50 monolayers examined) clearly indicate that the present fluorometric evaluation of monolayer fluorescence is reproducible, consistent in response to alterations in intracellular pH and consistent with quantitative measurements previously reported for single cells analyzed by microfluorometry (Helmle-Kolb et al., 1990*a*; Montrose & Murer, 1990*a*). In addition to the introduction of this new device to measure fluorometrically p*H*_i, we have determined in the present study some kinetic features of an apically located Na⁺/H⁺ exchanger in intact monolayers of OK cells. According to our experience a similar analysis by means of microfluorometry (i.e., single cell measurements) would be most difficult since variability in absolute transport rate from cell to cell is high, and not every experiment can be performed on the same cell "type." The present methodology overcomes this problem, yielding an average signal. Since the variability from preparation to preparation is much smaller than the variability from cell to cell, the present technique permits an accumulation of representative data in much shorter time.

In OK cells, steady-state p*H*_i was 7.68 ± 0.05 ($n = 20$) in HEPES-buffered Na-medium (p*H*_o = 7.4) in the absence of bicarbonate. This value is almost identical to that reported for OK cells examined by microfluorometry under bicarbonate-free conditions (Helmle-Kolb et al., 1990*a*; Montrose & Murer, 1990*b*). As it has been demonstrated previously, the mechanism of p*H*_i recovery in NH₄ prepulsed OK cells was strictly dependent on the addition of Na⁺ and was sensitive to EIPA in the perfusion medium (Helmle-Kolb et al., 1990*a*; Montrose & Murer, 1990*a*). Similar to our previous microfluorometric studies, the cellular recovery from an acid load in response to ordered addition of Na⁺ was shown to be a process that was predominant in the apical membrane of OK cells (Helmle-Kolb et al., 1990*a*; Montrose & Murer, 1990*a*). The findings of an apical Na⁺/H⁺ exchanger in OK cells are also in accordance with that reported in the rabbit and in the rat proximal tubule (Schwartz, 1981; Sasaki, Shiigai & Takeuchi, 1985; Alpern & Chambers, 1986; Kurtz, 1987). Finally, the experiment on PTH

inhibition of transport activity permits the conclusion that OK cells examined by the present perfusion technique demonstrate typical regulation of Na⁺/H⁺ exchange mechanism (Helmle-Kolb et al., 1990*a*), which may also be detected with the new technique. In the present paper we do not further address the mechanisms of PTH inhibition of Na⁺/H⁺ exchange, as this was done before by using either OK cells kept in suspension (Helmle-Kolb et al., 1990*b*) or OK cells grown on permeable support and analyzed at the single cell level (Helmle-Kolb et al., 1990*a*).

Our recent studies on regulation of Na⁺/H⁺ exchange in suspended cells have documented a p*H*_i dependence of the activity of the Na⁺/H⁺ exchanger (i.e., Na⁺/H⁺ exchange was activated greatly when the cytoplasm was acidified) (Helmle-Kolb et al., 1990*b*). A qualitative similar relationship of the increase in rate of Na⁺/H⁺ exchange as the p*H*_i becomes more acid is demonstrated in the present study. However, the absolute p*H*_i value at which exchange rate is projected to approach zero is close to 7.5. This value is higher than previously reported in suspended cells, but is similar to values reported using ²²Na⁺ flux in OK-cell monolayers (Tyler-Miller & Pollock, 1987). This may reflect differences in Na⁺/H⁺ exchange characteristics induced by the techniques used (OK cells in monolayer configuration *vs.* suspended cells), since the value measured under either condition is close to the respective resting p*H*_i value. The resting p*H*_i value at which in the present study Na⁺/H⁺ exchange is not detectable is well within the range of values reported by others (Frelin, Vigne & Lazdanski, 1985; Montrose & Murer, 1986; Renner et al., 1989), which are similarly close to the resting p*H*_i of the respective cell types studied. Furthermore, attaining a steady-state (resting) p*H*_i does not exclude the possibility that the exchanger is still operative. In considering the effect of p*H*_i decrease upon Na⁺ removal, which has been demonstrated in mesangial cells (Boyarsky et al., 1988; 1989), OK cells (Montrose & Murer, 1990*b*) and isolated perfused proximal tubules (Kurtz, 1987), it is possible that Na⁺-dependent H⁺ efflux can match H⁺ production by metabolism or H⁺ leak into the cell. Finally, it is of interest that a similar p*H*_i dependence of exchange activity as we have shown here has been demonstrated in other cell types (for review, *see* Frelin et al., 1988; Rothstein, 1989). Based on studies in renal microvillus membrane vesicles, this may be attributable to an allosteric activation of the exchanger by intracellular H⁺ (for review, *see* Aronson, 1985).

Our measurements of β in the absence of added bicarbonate illustrate that intrinsic intracellular buffer capacity is dependent on p*H*_i such that β increases as p*H*_i decreases. The findings that β in-

creases with low p*H*_i have been reported for several other cell types (e.g. Boyarsky et al., 1988; Renner et al., 1989; Weintraub & Machen, 1989). The observation that β increases with low p*H*_i together with a high Δp*H*_i/min at low p*H*_i implies that the Na⁺-dependent acid extrusion rate during p*H*_i recovery is highest at low p*H*_i values. We therefore have also calculated the rate of Na⁺-dependent transmembrane H⁺ flux (*J*^H) of OK cells. *J*^H was calculated according to the equation $J^H = dpH_i/dt \cdot \beta$ (where *dt* is assumed to be small compared to the p*H*_i-dependent change in β). When the p*H*_i sensitivity of the exchanger is analyzed either as Δp*H*_i/min or proton flux/min/liter cell water, the transporter is shown to increase transport rate at acidic p*H*_i values. A replot of the proton flux data indicate a strongly "sigmoidal" dependence of flux on intracellular proton concentration. The presence of a Hill coefficient >1 also suggests that more than one intracellular proton activates the transporter, but the absolute value of the Hill coefficient must be interpreted cautiously since we could not attain a [H⁺] giving *V*_{max} in these experiments (i.e., close to pH 6.0). Thus, the cellular mechanism of defense against acidification is reflected by both increase in buffer capacity and increase in Na⁺/H⁺ exchange rate, two components which act together to defend cellular pH.

The kinetic studies reported here indicate that p*H*_i has a marked effect on both the affinity and the activity of the Na⁺/H⁺ exchanger, such that both *K*_m and *V*_{max} increase as p*H*_i decreases. The current observations suggest that by lowering p*H*_i the Na⁺/H⁺ exchanger alters its properties from "high" affinity/low capacity to "low" affinity/high capacity, which under the conditions of cellular acid load might be also more efficient for proton extrusion. It has to be mentioned that the physiological extracellular Na⁺ concentration (and also in the proximal tubule) is around 140 mM, i.e., far above the apparent *K*_m values reported at either p*H*_i in the present study. The findings we report here are opposite to patterns of p*H*_i-induced alterations in Na⁺ activation kinetics of renal brush border membrane vesicles reported by Nord et al. (1984), which to our knowledge are the only studies where Na⁺ kinetics have been compared under pH equilibrium and proton gradient conditions. Nord and coworkers demonstrated that imposition of an outward H⁺ gradient at constant extracellular pH decreased *K*_m with only little change in *V*_{max}. The discrepancy between these former results and the present Na⁺/H⁺ exchange characteristics may be related to differences in experimental protocols used to examine Na⁺/H⁺ exchange activity. Nord and coworkers measured total Na⁺ flux (i.e., not the amiloride-sensitive or pH-driven component) and derived all kinetic param-

eters under conditions where they also had to "fit" a large diffusional component.

Inhibition by amiloride or its analogues has frequently been used to confirm Na⁺/H⁺ exchange (Frelin et al., 1988). Assuming that the only effect of EIPA is to inhibit Na⁺/H⁺ exchange, our data on inhibition of p*H*_i recovery rate as a function of the EIPA concentration indicate that Na⁺-dependent p*H*_i recovery is due to Na⁺/H⁺ exchange activity. The representation of EIPA inhibition of p*H*_i-stimulated Na⁺/H⁺ exchange in the Dixon plot suggests competition between Na⁺ and EIPA for binding to the Na⁺ site of the Na⁺/H⁺ exchanger. The *K*_i for EIPA derived from the plot was 3.4 μM.

In the present study we have described several properties of the Na⁺/H⁺ exchange system in a tissue culture model of renal origin. The use of the new perfusion technique has enabled a study of some kinetic features of apical Na⁺/H⁺ exchange to be quantified in monolayers of OK cells by routine spectrofluorometry. The characteristics of the OK-cell Na⁺/H⁺ exchanger reported here are very similar to those reported in microfluorometric studies. We present evidence for apical Na⁺/H⁺ exchange which is inhibited by PTH and EIPA. Inhibition kinetics for EIPA are competitive with external Na⁺. Rate of Na⁺/H⁺ exchange activity is stimulated by lowering p*H*_i. Rate of transport displays saturation with respect to external Na⁺, obeying the Michaelis-Menten equation. The interaction of extracellular Na⁺ with the exchanger is p*H*_i dependent. The relationship between extracellular [Na⁺] and p*H*_i is such that the affinity for Na⁺ is reduced by lower p*H*_i, whereas the apparent *V*_{max} is increased; thus, there is an apparent transition from "high affinity/low capacity" to "low affinity/high capacity" by a fall in p*H*_i.

We thank Denise Rossi for excellent secretarial assistance. This work was supported by the Swiss National Science Foundation (Grant Nr. 32-9486.88), the Stiftung für wissenschaftliche Forschung an der Universität Zürich, the Hartmann-Müller Stiftung, the Sandoz Stiftung, the Roche Research Foundation and the Geigy Jubiläums-Stiftung.

References

- Alpern, R.J. 1985. Mechanism of basolateral membrane H⁺/OH⁻/HCO₃⁻ transport in the rat proximal convoluted tubule. A sodium-coupled electrogenic process. *J. Gen. Physiol.* **86**:613-636
- Alpern, R.J., Chambers, M. 1986. Cell pH in the rat proximal convoluted tubule. Regulation by luminal and peritubular pH and sodium concentration. *J. Clin. Invest.* **78**:502-510
- Aronson, P.S. 1985. Kinetic properties of the plasma membrane Na⁺-H⁺ exchanger. *Annu. Rev. Physiol.* **47**:545-560
- Boron, W.F., DeWeer, P. 1976. Intracellular pH transients in

- squid giant axons caused by CO₂, NH₃, and metabolic inhibitors. *J. Gen. Physiol.* **67**:91–112
- Boyarsky, G., Ganz, M.B., Boron, W.F. 1989. Intracellular pH dependence of Na-H exchange and acid loading, and the effect of AVP, in mesangial cells examined in the absence of HCO₃⁻. In: The American Society of Nephrology, 22nd Annual Meeting (Washington, DC) Abstr. No.59
- Boyarsky, G., Ganz, M.B., Sterzel, R.B., Boron, W.F. 1988. pH regulation in single glomerular mesangial cells: I. Acid extrusion in absence and presence of HCO₃⁻. *Am. J. Physiol.* **255**:C844–C856
- Casavola, V., Helmle-Kolb, C., Murer, H. 1989. Separate regulatory control of apical and basolateral Na⁺/H⁺ exchange in renal epithelial cells. *Biochem. Res. Commun.* **165**:833–837
- Frelin, C., Vigne, P., Ladoux, A., Lazdunski, M. 1988. The regulation of the intracellular pH in cells from vertebrates. *Eur. J. Biochem.* **174**:3–14
- Frelin, C., Vigne, P., Lazdunski, M. 1985. The role of the Na⁺/H⁺ exchange system in the regulation of the internal pH in cultured cardiac cells. *Eur. J. Biochem.* **149**:1–4
- Haggerty, J.G., Agarwal, N., Reilly, R.F., Adelberg, E.A., Slayman, C.W. 1988. Pharmacologically different Na⁺/H⁺ antiporters on the apical and basolateral surfaces of cultured kidney cells (LLC-PK₁). *Proc. Natl. Acad. Sci. USA* **85**:6797–6801
- Helmle-Kolb, C., Montrose, M.H., Murer, H. 1990a. PTH-regulation of Na⁺/H⁺ exchange in opossum kidney cells: Polarity and mechanisms. *Pfluegers Arch. (in press)*
- Helmle-Kolb, C., Montrose, M.H., Stange, G., Murer, H. 1990b. Regulation of Na⁺/H⁺ exchange in opossum kidney cells by parathyroid hormone, cyclic AMP and phorbol esters. *Pfluegers Arch.* **415**:461–470
- Kurtz, I. 1987. Apical Na⁺/H⁺ antiporter and glycolysis-dependent H⁺-ATPase regulate intracellular pH in the rabbit S₃ proximal tubule. *J. Clin. Invest.* **80**:928–935
- Madshus, I.H. 1988. Regulation of intracellular pH in eukaryotic cells. *Biochem. J.* **250**:1–8
- Malmström, K., Stange, G., Murer, H. 1988. Intracellular cascades in the parathyroid-hormone-dependent regulation of Na⁺/phosphate cotransport in OK cells. *Biochem. J.* **251**:207–213
- Miller, R.T., Pollock, A.S. 1987. Modification of the internal pH sensitivity of the Na⁺/H⁺ antiporter by parathyroid hormone in a cultured renal cell line. *J. Biol. Chem.* **262**:9115–9120
- Montrose, M.H., Friedrich, T., Murer, H. 1987. Measurements of intracellular pH in single LLC-PK₁ cells: Recovery from an acid load via basolateral Na⁺/H⁺ exchange. *J. Membrane Biol.* **97**:63–78
- Montrose, M.H., Murer, H. 1986. Regulation of intracellular pH in LLC-PK₁ cells by Na⁺/H⁺ exchange. *J. Membrane Biol.* **93**:33–42
- Montrose, M.H., Murer, H. 1990a. Polarity and kinetics of Na⁺/H⁺ exchange in cultured opossum kidney (OK) cells. *Am. J. Physiol.* **259**:C121–C133
- Montrose, M.H., Murer, H. 1990b. Regulation of intracellular pH by cultured opossum kidney (OK) cells. *Am. J. Physiol.* **259**:C110–C120
- Nord, E.P., Brown, S.E.S., Crandall, E.D. 1988. Cl⁻/HCO₃⁻ exchange modulates intracellular pH in rat type II alveolar epithelial cells. *J. Biol. Chem.* **263**:5599–5606
- Nord, E.P., Hafezi, A., Wright, E.M., Fine, L.G. 1984. Mechanisms of Na⁺ uptake into renal brush border membrane vesicles. *Am. J. Physiol.* **247**:F548–F554
- Renner, E.L., Lake, J.R., Persico, M., Scharschmidt, B.F. 1989. Na⁺-H⁺ exchange activity in rat hepatocytes: Role in regulation of intracellular pH. *Am. J. Physiol.* **256**:G44–G52
- Rothstein, A. 1989. The Na⁺/H⁺ exchange system in cell pH and volume control. *Rev. Physiol. Biochem. Pharmacol.* **112**:235–257
- Sasaki, S., Shiigai, T., Takeuchi, J. 1985. Intracellular pH in the isolated perfused rabbit proximal tubule. *Am. J. Physiol.* **249**:F417–F423
- Schwartz, G.J. 1981. Na⁺-dependent H⁺ efflux from proximal tubule: Evidence for reversible Na⁺-H⁺ exchange. *Am. J. Physiol.* **241**:F380–F385
- Thomas, J.A., Buchsbaum, R.N., Zimniak, A., Racker, E. 1979. Intracellular pH measurements in Ehrlich ascites tumor cells utilizing spectroscopic probes generated *in situ*. *Biochemistry* **18**:2210–2218
- Vigne, P., Frelin, C., Cragoe, E.J., Lazdunski, M. 1983. Ethylisopropylamiloride: A new and highly potent derivative of amiloride for the inhibition of the Na⁺/H⁺ exchange system in various cell types. *Biochem. Biophys. Res. Commun.* **116**:86–90
- Vigne, P., Frelin, C., Cragoe, E.J., Lazdunski, M. 1984. Structure-activity relationships of amiloride and certain of its analogues in relation to the blockage of the Na⁺/H⁺ exchange system. *Mol. Pharmacol.* **25**:131–136
- Weintraub, W.H., Machen, T.E. 1989. pH regulation in heptoma cells: Roles for Na-H exchange Cl-HCO₃ exchange, and Na-HCO₃ cotransport. *Am. J. Physiol.* **257**:G317–G327

Received 17 July 1990; revised 26 September 1990